DISCUSSION ON SEISMICALLY TRIGGERED AVALANCHES ON MARS A. Lucas[1], I.J. Daubar[2], M. Le Teuff[1], L. V.Posiolova[3], G. Sainton[1], A. Mangeney[1], C. Perrin[4], T. Kawamura[1], D. Giardini[5], P. Lognonné[1] [1]Université Paris Cité, IPGP, CNRS, France, [2]Univ of AZ-Planetary Sciences, USA, [3]Malin Space Science Systems, CA, USA, [4]Laboratoire de Planétologie et Géosciences, CNRS, Nantes Université, France, [5]ETH Zurich, Department of Earth Sciences, Institute of Geophysics, Switzerland, (lucas@ipgp.fr)

Motivation: On May 5, 2022, the martian SEIS seismometer recorded an unprecedented M_W^{Ma}4.7 Marsquake. The epicenter is located at 3.0°S, 171.9°E. The areas is barely flat with only a few N-S tectonic-like features. Most unfilled impact craters and ridges show dust avalanches (a.k.a. Slope streaks). We investigate the post-seismic outcomes in terms of avalanche triggering under today's Mars conditions in the framework of the s1222a event.

Methods: Using orbital images from CTX and HiRISE cameras, both onboard MRO spacecraft, we investigate all CTX and HiRISE images around ± 8° away from the estimated epicenter. We completed this data set with both MOC and visible THEMIS data. Hence, we mapped all observable avalanches over the 2005–2022 period. We requested dedicated new orbital observations targeted towards the most favorable areas for avalanches from our initial mapping (Fig. 1).

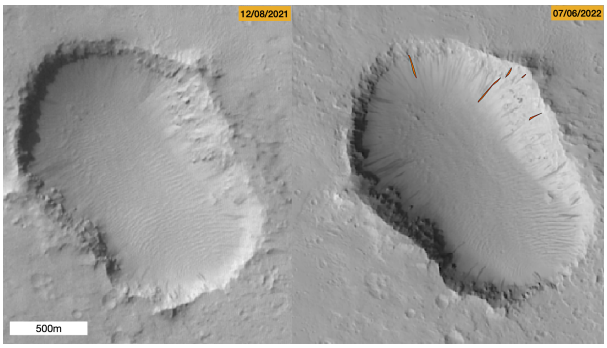

Figure 1: Post-event avalanches observed on a 10 months span CTX/HiRISE pair.

In addition to imagery, we integrated additional orbital data such as elevation (from MOLA and HRSC) as well as thermal inertial from THEMIS sensor onboard Odyssey. The collected observations are summarized in the Figure 3. For each available pairs of images we computed the avalanche rate as defined $q_{ava} = \Delta n/(A \times \Delta t)$, where Δn is the number of new avalanches between two images, A being the areas of the slopes where avalanches are seen over 2005–2022 period, and Δt being the time expressed in martian year between the two images. A is obtained from heatmap avalanche density computed from the total mapping (Fig. 3).

Results: Thanks to the high resolution imagery, almost 4500+ avalanches have been identified in the area of interest. About 200 new avalanches have been detected over the 2005–2021 period. As for today, about 100 avalanches are detected on the post s1222a event images with respect to their 2005–2021 period counterparts. Consequently, not all of these can be dated after the event, nor being associated with it. Most avalanches are seen inside impact crater walls, which are the main topographical features presenting steep slopes. Pre-event nominal avalanche rate $q_{ava} = 5_1^{30}$ km^{-2}.MYr^{-1} (Fig. 2).

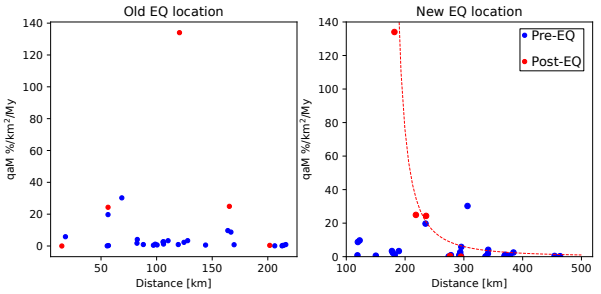

Figure 2: Avalanche rate as a function of EQ location and respective epicentral distance.

Interestingly, when considering the initial location estimate of the marsquake (yellow star on Fig. 3), the post-event avalanche rate q_{ava} does not show any specific pattern (Fig. 2-left). When now considering the new position, evaluated from body waves [1], the q_{ava} follow a well known trend. Indeed, one can relate ground deformation with avalanche rate. Following previous approaches [2, 3], we can relate the ground motion with epicentral distance Δ through:

$$G(\Delta) = \frac{K}{(\alpha + \Delta/D)^n}, \quad (1)$$

where K and α are empirical parameters, and with n = {2,1.7,1.5} for the acceleration, velocity and displacement respectively [3]. This leads to evaluate the new EQ location with respect to the avalanche rates as a function of the epicentral offset with $n = 2$ (Fig. 2-right).

Discussion: When considering the hypothesis of seismic induced avalanches, it is important to discuss the absence of new avalanches along some steep slopes (where

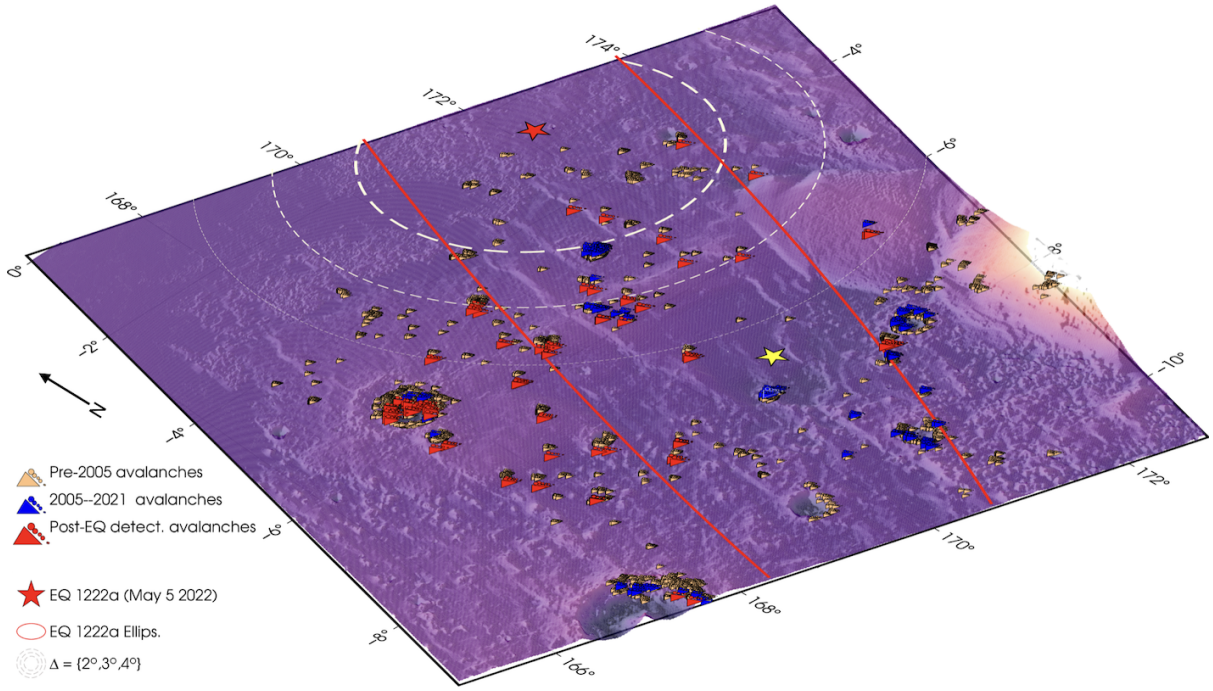

Figure 3: Mapping summary of avalanches around marsquake s1222a.

previous avalanches are seen) on the post-event imagery. A few locations are noted on Figure 3. On Earth, it is well known that not only the epicentral distance to an earthquake controls the induced mass wasting triggering.

On Mars, subsurface properties can be derived through the thermal inertial, which is the related to how solar energy is absorbed and resulting heat propagates within the subsurface. Hence this is strongly correlates with the material properties as $\Gamma \equiv \sqrt{\kappa_e(1-p)\rho C(T)}$, where κ_e is the effective thermal conductivity, p the porosity, ρ the density and $C(T)$ specific heat capacity. So, we observe that avalanches are formed mostly over low thermal inertia terrains, which correspond to unconsolidated terrains, and/or granular material (Fig. 4).

On one hand, when thermal inertial is high (i.e., $\Gamma >$ 400 S.I.) the post event rate is not higher that the pre-event period. On the other hand, when thermal inertial is low (i.e., $\Gamma << 400$ S.I.) the post event rate is higher.

To summarize, as on Earth, seismic activity with favorable geology may be responsible for triggering avalanches on Mars.

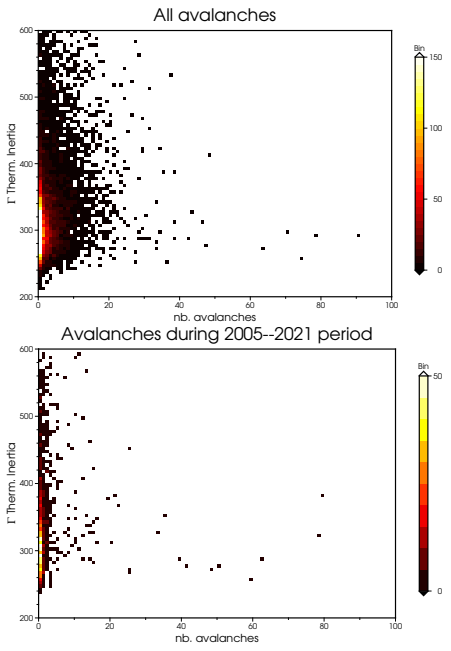

Figure 4: Thermal inertia of avalanche terrain from full data (top) and where new avalanches occurred during 2005-2021 (bottom).

References: **[1]** T. Kawamura et al. "S1222a - the largest Marsquake detected by InSight". In: *Geophysical Research Letters* (2023). **[2]** J. Gomberg et al. "Earthquake Dynamic Triggering and Ground Motion Scaling". In: *The 4th International Workshop on Statistical Seismology* (2006). **[3]** Joan Gomberg and Karen Felzer. "A model of earthquake triggering probabilities and application to dynamic deformations constrained by ground motion observations". In: *Journal of Geophysical Research: Solid Earth* 113.B10 (2008).